

Accepted Manuscript

Development of novel nano-biocomposite antioxidant films based on poly (lactic acid) and thymol for active packaging

Marina Ramos, Alfonso Jiménez, Mercedes Peltzer, María C. Garrigós

PII: S0308-8146(14)00571-8
DOI: <http://dx.doi.org/10.1016/j.foodchem.2014.04.026>
Reference: FOCH 15687

To appear in: *Food Chemistry*

Received Date: 10 September 2012
Revised Date: 27 March 2014
Accepted Date: 5 April 2014

Please cite this article as: Ramos, M., Jiménez, A., Peltzer, M., Garrigós, M.C., Development of novel nano-biocomposite antioxidant films based on poly (lactic acid) and thymol for active packaging, *Food Chemistry* (2014), doi: <http://dx.doi.org/10.1016/j.foodchem.2014.04.026>

This is a PDF file of an unedited manuscript that has been accepted for publication. As a service to our customers we are providing this early version of the manuscript. The manuscript will undergo copyediting, typesetting, and review of the resulting proof before it is published in its final form. Please note that during the production process errors may be discovered which could affect the content, and all legal disclaimers that apply to the journal pertain.



1 **Development of novel nano-biocomposite antioxidant films based on poly (lactic**
2 **acid) and thymol for active packaging**

3
4 Marina Ramos*, Alfonso Jiménez, Mercedes Peltzer, María C. Garrigós

5 Analytical Chemistry, Nutrition & Food Sciences Department, University of Alicante

6 P.O. Box 99, 03080. Alicante, Spain

7 Corresponding author. Tel. +34965903400x1187; fax. +34965903697.

8 E-mail address: marina.ramos@ua.es (M. Ramos)

9
10 **Abstract**

11 Novel nano-biocomposite films based on poly (lactic acid) (PLA) were prepared by
12 incorporating thymol, as the active additive, and modified montmorillonite (D43B) at
13 two different concentrations. A complete thermal, structural, mechanical and functional
14 characterization of all nano-biocomposites was carried out. Thermal stability was not
15 significantly affected by the addition of thymol, but the incorporation of D43B
16 improved mechanical properties and reduced the oxygen transmission rate by the
17 formation of intercalated structures, as suggested by wide angle X-ray scattering
18 patterns and transmission electron microscopy images. The addition of thymol
19 decreased the PLA glass transition temperature, as the result of the polymer
20 plasticization, and led to modification of the elastic modulus and elongation at break.
21 Finally, the amount of thymol remaining in these formulations was determined by liquid
22 chromatography (HPLC-UV) and the antioxidant activity by the DPPH spectroscopic
23 method, suggesting that the formulated nano-biocomposites could be considered a
24 promising antioxidant active packaging material.

25
26 **Keywords:** PLA; active packaging; thymol; montmorillonite; antioxidant film.

27

28 **Introduction**

29 Poly (lactic acid) (PLA) is one of the most important commercially available bio-
30 based and biodegradable thermoplastic polyesters (Inkinen, Hakkarainen, Albertsson &
31 Sodergard, 2011). PLA can offer a sustainable alternative for food packaging across a
32 wide range of commodity applications in response to consumers' demands and market
33 trends in the use of renewable resources (Hughes, Thomas, Byun & Whiteside, 2012).
34 PLA is a highly transparent and rigid material with a relatively low crystallization rate,
35 making it a promising candidate for the fabrication of biaxial oriented films,
36 thermoformed containers and stretch-blown bottles (Inkinen et al., 2011). However,
37 some characteristic properties of pure PLA are inadequate for food packaging
38 applications, such as weak thermal stability, low glass transition temperature, low gas
39 barrier properties, and low ductility and toughness (Hwang et al., 2012). Recently, these
40 poor PLA intrinsic properties have been improved by the reinforcement of the polymer
41 matrix with layered silicates (Fukushima, Tabuani & Camino, 2009b; Gamez-Perez et
42 al., 2011; Lagaron & Lopez-Rubio, 2011; Picard, Espuche & Fulchiron, 2011). In this
43 sense, the incorporation of lamellar nanofillers with high aspect ratio, such as
44 montmorillonites, has significantly enhanced mechanical, gas barrier, and optical
45 properties (Rhim, Hong & Ha, 2009).

46 Current innovations in food packaging research include the development of active
47 packaging systems based on materials, which can include a variety of additives such as
48 antioxidants, antimicrobials, vitamins, flavours and colorants with the aim of improving
49 their appearance and to extend foodstuff shelf-life (Álvarez, 2000; Del Nobile, Conte,
50 Buonocore, Incoronato, Massaro & Panza, 2009; Gómez-Estaca, Giménez, Montero &
51 Gómez-Guillén, 2009). The increasing demand for natural additives has resulted in

52 studies based on natural active compounds, such as plant extracts or essential oils,
53 which are categorized as Generally Recognised as Safe (GRAS) by the US Food and
54 Drug Administration as well as the current European Legislation for materials intended
55 to be in contact with food (EU N10/2011 Regulation) (Ramos, Jiménez, Peltzer &
56 Garrigós, 2012).

57 The addition of natural antioxidant additives allows their continued release during
58 storage and distribution, extending food shelf-life by decreasing lipid auto-oxidation,
59 which is recognized as a major cause of deterioration affecting both sensory and
60 nutritional quality (Manzanarez-López, Soto-Valdez, Auras & Peralta, 2011). In this
61 sense, thymol is a phenolic compound obtained from thyme and oregano essential oils
62 that has been reported to be an effective antioxidant to reduce or eliminate lipid
63 oxidation (Al-Bandak & Oreopoulou, 2007). Thymol antioxidant properties are due to
64 its ability to donate H-atoms from phenol hydroxyl groups, which could react with
65 peroxy radicals to produce stabilized phenoxyl radicals and, consequently, terminate
66 lipid peroxidation chain reactions (Mastelic et al., 2008; Viuda-Martos, Navajas,
67 Zapata, Fernández-López & Pérez-Álvarez, 2010). Several methods can be used to
68 evaluate the antioxidant activity of natural additives as pure compounds or plant
69 extracts, which are based on the measurement of the free radical scavenging ability
70 (Sánchez-Moreno, 2002).

71 The development of different nanocomposites based on PLA with nanoclays
72 (Fukushima et al., 2009b; Gamez-Perez et al., 2011; Picard et al., 2011) or active
73 additives (Byun, Kim & Whiteside, 2010; López-Rubio & Lagaron, 2010; Hwang et al.,
74 2012) has been extensively reported by several authors in the last years. However, few
75 works have reported the combination of natural active additives and nanofillers in
76 biopolymer matrices resulting in nano-biocomposites with antioxidant properties and

77 functionalities for use in food packaging applications. The use of these materials could
78 be a promising alternative to enhance mechanical and gas barrier properties and extend
79 foodstuff shelf-life.

80 This study focused on the development of antioxidant biodegradable films based on
81 PLA reinforced with an organically modified montmorillonite [Dellite 43B (D43B)] and
82 a natural additive (thymol) to obtain nano-biocomposites based on renewable resources
83 with antioxidant activity and enhanced properties for active packaging applications. A
84 full characterization was carried out including the determination of thermal, structural,
85 mechanical and functional properties. Finally, the presence of thymol in the nano-
86 biocomposites was determined by HPLC-UV analysis and antioxidant activity assessed
87 by using the DPPH method.

88

89 **1. Materials and methods**

90

91 1.1. Materials

92 Poly (lactic acid) (PLA) 4060D was purchased in pellets from Natureworks Co.,
93 (Minnetonka, MN, USA). Thymol (99.5 %), 2,2-Diphenyl-1-picrylhydrazyl (DPPH,
94 95%) and methanol (HPLC grade) were supplied by Sigma-Aldrich (Madrid, Spain).

95 The nanoclay used was Dellite®43B (D43B) (Laviosa Chimica Mineraria S.p.A.
96 Livorno, Italy). This nanoclay is a dimethyl-benzylidihydrogenated tallow ammonium
97 modified montmorillonite; and it has a cation exchange capacity (CEC) of 95 meq/100 g
98 clay, a bulk density of 0.40 g cm^{-3} and a typical particle size distribution between 7-9
99 μm .

100

101 1.2. Nano-biocomposites preparation

102 The different nano-biocomposites were obtained by melt-blending in a Haake
103 Polylab QC mixer (ThermoFischer Scientific, Walham, MA, USA) with a mixing time
104 of 20 min at 160 °C. Two different rotor speeds were used: 150 rpm in the loading and
105 mixing steps and 100 rpm for the last 5 min, when thymol was added in order to limit
106 degradation and to ensure the presence of the active additive in the final blends. Prior to
107 the mixing step, PLA and the nanoclay were dried for 24 h at 80 °C and 100 °C,
108 respectively. Thymol was used as received.

109 Five different formulations were obtained by adding thymol at one concentration
110 level (8 wt%) and D43B at two different loadings (2.5 and 5 wt%), as described in
111 Table 1. An additional sample without any additive was also prepared and used as
112 control (neat PLA).

113 Films were obtained by compression-moulding at 180 °C in a hot-plates press
114 (Carver Inc 3850, Wabash, IN, USA). Blends were kept at atmospheric pressure for 5
115 min until melted and pressed at 2 MPa for 1 min, 3.5 MPa for 1 min and finally 5 MPa
116 for 5 min to eliminate the trapped air bubbles. Transparent films were obtained with
117 average thickness $210 \pm 1 \mu\text{m}$ measured with a Digimatic Micrometer Series 293 MDC-
118 Lite (Mitutoyo, Japan) at five random positions.

119

120 2.3. Thymol quantification

121 The actual amount of thymol in PLA films after processing was determined by solid-
122 liquid extraction followed by liquid chromatography coupled to ultraviolet spectroscopy
123 (HPLC-UV) analysis. 0.05 ± 0.01 g of each film were extracted with 10 mL of methanol
124 at 40 °C and 50 % relative humidity (RH) for 24 h in a climate chamber (Dycometal
125 CM-081, Barcelona, Spain), as previously reported (Manzanarez-López et al., 2011).

126 Thymol was determined with a Shimadzu LC-20A liquid chromatograph (Kyoto,
127 Japan) equipped with a UV detector at 274 nm. The column used was a LiChrospher
128 100 RP 18 (250 mm x 5 mm x 5 μm , Agilent Technologies, USA). The mobile phase
129 was composed of acetonitrile and water (40:60) at 1 mL min^{-1} flow rate. 20 μL of the
130 extracted samples were injected and analyses were performed in triplicate.
131 Quantification of the active additive was carried out by comparison of the
132 chromatographic peak areas with standards in the same concentration range. Calibration
133 curves were run at five concentrations from 100-500 mg Kg^{-1} using appropriately
134 diluted standards of thymol in methanol.

135 The antioxidant activity of thymol was analyzed using the stable radical 2,2-
136 diphenyl-1-picrylhydrazyl (DPPH) as previously reported (Byun et al., 2010). This
137 method is based on colour decay when the odd electron of the nitrogen atom in the
138 DPPH radical is reduced by receiving one hydrogen atom from antioxidant compounds
139 (Scherer & Godoy, 2009).

140 500 μL of extracts were mixed with 2 mL of a methanolic solution of DPPH (0.06
141 mM) in a capped cuvette. The mixture was shaken vigorously at room temperature and
142 the absorbance of the solution was measured at 517 nm with a Biomate-3 UV-VIS
143 spectrophotometer (Thermospectronic, Mobile, AL, USA). DPPH radical absorbs at 517
144 nm but, upon reduction, its absorption at this particular wavelength decreases. The
145 decay in absorbance was measured at 1 min intervals until it was stabilized (200 min).

146 All analyses were performed in triplicate.

147 The scavenging ability of the stable radical DPPH was calculated as percentage of
148 inhibition (I %) with the equation (1):

$$149 \quad I(\%) = [(A_{Control} - A_{Sample}) / A_{Control}] \cdot 100 \quad (1)$$

150

151 where $A_{Control}$ is the absorbance of the blank sample at $t = 0$ min and A_{Sample} is the
152 absorbance of the tested sample at $t = 200$ min.

153

154 2.4. Thermal analysis

155 Thermogravimetric analysis (TGA) tests were performed with a TGA/SDTA 851
156 Mettler Toledo thermal analyzer (Schwarzenbach, Switzerland). Approximately 5 mg
157 samples were heated from 30 °C to 700 °C at 10 °C min⁻¹ under nitrogen (flow rate 50
158 mL min⁻¹).

159 Differential scanning calorimetry (DSC) tests were used to determine glass transition
160 temperatures (T_g) of all materials using a TA DSC Q-2000 instrument (New Castle, DE,
161 USA) under nitrogen atmosphere (flow rate 50 mL min⁻¹). 3 mg samples were heated
162 from -30 °C to 200 °C at 10 °C min⁻¹ (3 min hold), then cooled at 10 °C min⁻¹ to -30 °C
163 (3 min hold) and further heating to 200 °C at 10 °C min⁻¹.

164

165 2.5. Mechanical properties

166 Tensile properties of all films were determined with a 3340 Series Single Column
167 System Instron Instrument, LR30K model (Fareham Hants, UK) equipped with a 2 kN
168 load cell. The main tensile parameters, such as elastic modulus and elongation at break,
169 were calculated from stress-strain curves according to ASTM D882-09 Standard
170 procedure (ASTM D 882 - 09. 2009). Before testing, all samples were conditioned for
171 48 h at 25 °C and 50 % RH. Tests were performed with 100 x 10 mm² rectangular
172 probes and initial grip separation of 60 mm. The specimens were stretched at 10 mm
173 min⁻¹ until breaking. Results were the average of five measurements (\pm standard
174 deviation).

175

176 2.6. Oxygen transmission rate (OTR)

177 OTR is defined as the quantity of oxygen circulating through a determined area of
178 the parallel surface of a plastic film per time unit. An oxygen permeation analyzer (8500
179 model Systech, Metrotec S.A, Spain) was used for OTR tests. Pure oxygen (99.9%) was
180 introduced into the upper half of the diffusion chamber while nitrogen was injected into
181 the lower half, where an oxygen sensor was located. Films were cut into 14 cm diameter
182 circles for each formulation and they were clamped in the diffusion chamber at 25 °C
183 before testing. Tests were performed in triplicate and mean values were expressed as
184 oxygen transmission rate per film thickness (OTR·e).

186 2.7. Colour tests

187 Colour modifications on PLA films caused by the addition of the active additive and
188 the nanoclay were followed by using a Konica CM-3600d COLORFLEX-DIFF2
189 colorimeter, HunterLab, (Reston, VA, USA). Colour values were expressed as L*
190 (lightness), a* (red/green) and b* (yellow/blue) coordinates in the CIELab colour space.
191 These parameters were determined at five different locations in films surfaces and the
192 average values were calculated. Total colour difference (ΔE^*) was calculated according
193 to Eq. (2).

$$195 \Delta E^* = [(\Delta L^*)^2 + (\Delta a^*)^2 + (\Delta b^*)^2]^{1/2} \quad (2)$$

196
197 where ΔL^* , Δa^* and Δb^* are the coordinate differences between control (neat PLA) and
198 samples.

200 2.8. Morphological analysis

201 The nano-biocomposites structure, including the nanoclay dispersion, was studied by
202 wide angle X-ray scattering (WAXS) patterns and transmission electron microscopy
203 (TEM) micrographs.

204 WAXS patterns were recorded at room temperature in the scattering angle (2θ) 2-30°
205 (step size: 0.01°, scanning rate: 8 s step⁻¹) using filtered Cu K α radiation (λ : 1.54 Å). A
206 Bruker D8-Advance model diffractometer (Madison, WI, USA) was used to determine
207 the interlayer distance (d-spacing) and intercalation of the nanoclay.

208 TEM micrographs were performed using a JEOL JEM-2010 (Tokyo, Japan) with
209 accelerating voltage 100 kV. Prior to analysis, films were ultra-microtomed to obtain
210 slices of 100 nm thick (RMC, model MTXL).

211

212 **3. Results and discussion**

213

214 3.1. Determination of thymol in nano-biocomposite films and antioxidant activity

215 The amount of thymol present in formulations after processing is indicated in Table
216 1. Results showed that approximately 30 % of the initially thymol was lost during
217 processing by evaporation or degradation due to the high temperature used during the
218 polymer melting (Ramos et al., 2012). In this sense, other commonly used antioxidants
219 in PLA-based formulations, such as butylated hydroxytoluene (BHT), suffer similar
220 losses due to several factors, such as poor mixing in the extruder, evaporation, thermal
221 degradation and the own antioxidant action of BHT to protect the polymer during
222 processing (Ortiz-Vazquez, Shin, Soto-Valdez & Auras, 2011). Antioxidant volatility is
223 desirable for food packaging to promote their migration from the polymer surface
224 (Wessling, Nielsen, & Giacini, 2001). Therefore, thymol can be considered a good
225 antioxidant in food packaging materials since most remains after processing and may be

226 released from the polymer matrix to improve food shelf-life. On the other hand, the
227 amount of thymol after processing was slightly higher in nanocomposites containing
228 D43B because the nanoclay can retard thymol evaporation during processing.

229 The antioxidant activity of the extracts obtained was estimated by scavenging
230 activity against DPPH radicals. This test was performed to evaluate if the remaining
231 thymol in the polymer matrix was enough to be considered an efficient antioxidant in
232 these formulations. Results are also shown in Table 1. All extracts containing thymol
233 showed an important antioxidant activity, as determined by the inhibition of the DPPH
234 radical. The inhibition values are indicative of the amount of thymol remaining in the
235 polymer matrix, which is able to act as an active (antioxidant) agent. In addition, thymol
236 could protect the polymer matrix from oxidative degradation during processing and
237 further the use of these nano-biocomposites (Ramos et al., 2012).

238

239 **Table 1**

240

241 3.2. Thermal analysis

242 Many authors have considered several molecular, as well as radical, mechanisms to
243 explain PLA thermal degradation. The primary cause reported is a non-radical,
244 'backbiting' ester interchange reaction involving -OH chain ends. This reaction
245 mechanism can, depending upon the size of the cyclic transition state, produce lactide,
246 oligomers or acetaldehyde as well as carbon monoxide. However, other authors have
247 proposed radical reactions, which start with either alkyloxygen or acyl-oxygen
248 homolysis leading to the formation of several types of oxygen- and carbon-centred
249 macroradicals and carbon monoxide (Fukushima, Abbate, Tabuani, Gennari & Camino,
250 2009a).

251 The thermal stability of all the materials was studied by TGA under nitrogen. Fig. 1
252 shows the weight loss (TG) and derivative curves (DTG) obtained for PLA and all
253 nano-biocomposites. The main degradation peak for PLA was observed in all samples
254 around 365-370 °C. The first degradation step observed in those materials containing
255 thymol was at 120 °C and continued up to 280 °C. Losses were associated with thymol
256 degradation, as reported in previous works (Ramos et al., 2012). This result is another
257 indication of the presence of thymol after processing. In this sense, the amounts of
258 thymol, calculated by TGA (Table 2), were similar in all cases to values obtained from
259 the quantification study discussed in the previous section. The initial degradation
260 temperature (T_{ini}), determined at 5% of weight loss, and maximum degradation
261 temperature (T_{max}) of the PLA degradation process are also shown in Table 2. No
262 noticeable differences were observed for T_{ini} and T_{max} values in the materials studied.
263 These results showed the addition of thymol and D43B did not significantly affect the
264 nano-biocomposites thermal degradation profile.

265

266 **Fig. 1**

267

268 Glass transition temperatures (T_g) in all nano-biocomposites were determined by
269 DSC (Table 2). This parameter is dependent upon the polymer structural arrangement
270 and corresponds to the torsion oscillation of the carbon backbone (Hughes et al., 2012).
271 T_g results showed the addition of D43B to PLA did not produce significant changes in
272 the polymer structure, as reported by other authors (Lewitus, McCarthy, Ophir & Kenig,
273 2006). The effect of thymol on PLA was much more important; thymol caused a
274 decrease of more than 10 °C in T_g values, regardless of the presence of D43B. Similar
275 behaviour was reported in PLA formulations with other antioxidants (Byun, Kim &

276 Whiteside, 2010; Hwang et al., 2012). This could be explained by the plasticizing effect
277 caused by thymol resulting in an increase in molecular mobility of the macromolecular
278 chains. Parameters related with crystallization or melting phenomena of PLA nano-
279 biocomposites were not observed in these formulations due to the amorphous structure
280 of the PLA used in this study.

281

282 **Table 2**

283

284 3.3. Mechanical properties

285 The addition of nanoclays to polymer matrices usually improves mechanical
286 properties, particularly when nanoclay exfoliation occurs. Tensile tests were performed
287 with all the materials studied to evaluate the influence on ductile properties. Results
288 from elastic modulus (MPa) and elongation at break (%) are shown in Table 3. The
289 addition of thymol to PLA matrices resulted in slight modifications of tensile properties.
290 Elastic modulus decreased around 15 % from the original values for neat PLA for those
291 materials containing thymol. This modification could be explained, again, by the
292 plasticizing effect caused by thymol. This result confirmed the observed decrease in T_g
293 values already reported. Similar results have been reported for PLA and low-density
294 polyethylene (LDPE) formulations with active compounds, such as resveratrol,
295 carvacrol or α -tocopherol (Hwang et al., 2012; Persico, Ambrogi, Carfagna, Cerruti,
296 Ferrocino & Mauriello, 2009).

297

298 **Table 3**

299

300

301 As expected, the addition of D43B to PLA increased the elastic modulus and
302 decreased elongation at break. Therefore, the addition of nanoclays increased brittleness
303 (Tabatabaei & Aji, 2011). This behaviour is related to reinforcement provided by
304 silicate layers and the high aspect ratio and surface area, good dispersion of clay layers
305 throughout the polymer matrix, and strong interactions (Quilaqueo Gutiérrez,
306 Echeverría, Ihl, Bifani & Mauri, 2012). However, this effect was not observed for
307 ternary nano-biocomposites, where lower elastic modulus values were observed
308 compared with pure PLA. This suggests the plasticizing effect of thymol in PLA may
309 prevail over the reinforcement offered by the nanoclay.

310

311 3.4. Oxygen transmission rate (OTR)

312 Barrier properties to oxygen of PLA nano-biocomposites were studied by the
313 determination of oxygen transmission rate per film thickness (e), $OTR \cdot e$. Results are
314 shown in Table 3. A slight decrease in $OTR \cdot e$ values for films containing D43B was
315 observed. These results could be attributed to the effective intercalation of the nanoclay
316 into the PLA matrix. This behaviour can be explained by considering that oxygen
317 transmission rate is governed by two mechanisms: diffusion and sorption. In general,
318 the efficient dispersion of D43B into the polymer matrix may form a tortuous pathway
319 for oxygen molecules to permeate through the film. This more tortuous pathway results
320 in oxygen molecules following a more complicated way through the polymer matrix. In
321 general, the efficient dispersion of D43B into the polymer matrix may form a tortuous
322 pathway for oxygen molecules to permeate through the film (Martino, Ruseckaite,
323 Jiménez & Averous, 2010; Quilaqueo Gutiérrez et al., 2012).

324

325 Regarding PLA with thymol, a slight increase in the $OTR \cdot e$ value was observed. The
326 addition of thymol could modify the properties of PLA by increasing the mobility of
327 macromolecular chains, reducing the polymer orientation and, consequently, decreasing
328 oxygen permeability (Jamshidian, Arab Tehrani, Cleymand, Leconte, Falher &
329 Desobry, 2012).

330 Finally, no significant differences were found in $OTR \cdot e$ values for samples
331 PLA/D43B2.5 and PLA/T/D43B2.5, containing D43B and thymol. However, sample
332 PLA/T/D43B5 presented an $OTR \cdot e$ value near to that obtained for PLA and higher than
333 the one observed for sample PLA/D43B5, which may be due to decreased oxygen
334 permeability caused by incorporation of thymol.

335 In general, the use of nanoclays in these PLA nano-biocomposites effectively
336 improved oxygen barrier properties for food packaging applications.

338 3.5. Optical properties

339 Colour and transparency are important factors to be considered in food packaging
340 since they could influence consumer acceptance and commercial success of a food
341 product. Fig. 2 shows the visual aspect of all formulations. All the films had high
342 transparency. Moreover, no agglomeration effects were revealed confirming the
343 efficiency of the processing of PLA nanocomposites. However, some differences in the
344 CIELab coordinates (L^* , a^* , b^*) and ΔE^* between neat PLA and nanocomposites were
345 observed (Table 3). These differences could be attributed to the intrinsic colour of the
346 additives used (white for thymol and yellowish for D43B). In this sense, pure PLA had
347 the lowest L^* value, indicating that brightness increased with the addition of thymol and
348 D43B. A yellowish-reddish tone was obtained for PLA/T, while PLA/T/D43B5 showed
349 the higher value for ΔE^* , as expected, due to the high concentrations of the additives

350 used (5 wt% D43B and 8 wt% thymol). The uniform distribution of the colour observed
351 throughout the films (Fig. 2) also implies the additives were distributed uniformly
352 within the polymer matrix. Similar tendencies in colour differences have been reported
353 when using active additives such as α -tocopherol and resveratrol into PLA, where the
354 presence of these compounds contributed to strength of colour of the films obtained
355 (Byun et al., 2010).

356

357 **Fig. 2**

358

359 3.6. Morphological analysis

360 3.6.1. Wide Angle X-Ray scattering (WAXS)

361 WAXS is a useful technique to determine d-spacing in intercalated nanocomposites.
362 The WAXS pattern of PLA is characterized by a broad peak approximately at $2\theta = 15^\circ$
363 (Fukushima et al., 2009a), confirming its amorphous structure. No significant
364 differences were found from the WAXS patterns of all the formulations studied at this
365 angle range, indicating the polymer structure and crystallinity were not influenced by
366 the presence of D43B and/or thymol.

367 The most significant features in this study were found in the low angle range ($2-10^\circ$),
368 (Figure 3). D43B is characterized by a single diffraction peak at $2\theta = 4.6^\circ$
369 corresponding to the (001) plane, accounting for a 19.2 \AA interlayer distance. A shift of
370 the clay diffraction peak to lower angles, corresponding to an interlayer distance of 35.6
371 \AA , was observed for all nano-biocomposites suggesting good interaction of D43B with
372 the polymer matrix. Moreover, a significant decrease in peak intensity was observed,
373 accounting for the formation of a disordered structure. These results indicate the
374 formation of intercalated nano-biocomposites with PLA chains in the galleries of the

375 D43B layers (Picard et al., 2011). The basal diffraction observed at 2θ around 5.2° (d-
376 spacing = 17.0 \AA) in the nano-biocomposites WAXS patterns could be attributed to the
377 fraction characterized by a different alkylammonium chain arrangement in the interlayer
378 space (Persico et al., 2009).

379 The lowest peak intensity in the WAXS study was obtained for PLA/T/D43B2.5.
380 The presence of thymol could favour nanoclay exfoliation and the effective interaction
381 between the silicate layers and thymol, which could promote the swelling of the
382 nanoclay stacks (Persico et al., 2009). However, the formulations with 5 wt% of D43B
383 showed more intense peaks. This behaviour could be due to the unfavourable effect of
384 nanoclay swelling, produced by thymol at high nanoclay loading. In conclusion, WAXS
385 results suggest effective nanoclay intercalation achieved by mixing PLA with 2.5 wt%
386 of D43B and 8 wt% of thymol.

387

388 **Fig. 3**

389

390 3.6.2. Transmission Electron Microscopy (TEM)

391 The dispersion of nanoclays in PLA nano-biocomposites was evaluated by TEM.
392 Figure 4 shows the micrographs obtained for PLA/T/D43B2.5, showing the
393 nanoparticles partial exfoliation. Single dispersed clay layers (dark regions in Figure 3)
394 were randomly distributed through the PLA matrix (clear areas) and some regions with
395 complete exfoliation of nanoclay layers were noticed. TEM analyses also suggested the
396 good dispersion of D43B and thymol through the PLA matrix, already asserted by
397 WAXS patterns, since no important aggregates were observed. The interaction of
398 nanoclays with PLA was attributed to the formation of hydrogen bonds between the

399 carbonyl group of lactide and the hydroxyl groups of the nanoclay organic modifier
400 (Fukushima et al., 2009b).

401

402 **Fig. 4**

403

404 **4. Conclusions**

405 Different nano-biocomposite films, based on PLA, with antioxidant potential to be
406 used in active packaging were processed and characterized. Several analytical
407 techniques were used to evaluate the effects of incorporating the nanoclay (D43B) and
408 thymol on the PLA nano-biocomposites properties. The addition of thymol did not
409 significantly affect the thermal stability of PLA, but some decrease in the elastic
410 modulus was observed due to the thymol plasticizing effect. The incorporation of D43B
411 resulted in a clear enhancement of oxygen barrier and mechanical properties, due to the
412 intercalation and partial exfoliation of the nanoparticles through the polymer matrix.
413 Some differences in films colour were observed with the addition of thymol and D43B,
414 but films remained mostly transparent. Most of the thymol added remained in the
415 formulations after processing, which resulted in a significant antioxidant activity, as
416 indicated by the high percentage of inhibition obtained using the DPPH test. In
417 conclusion, the PLA nano-biocomposites studied, in particular those containing 8 wt%
418 of thymol and 2.5 wt% of D43B, could be considered promising antioxidant active
419 packaging materials with a biodegradable nature and able to increase foodstuff shelf-
420 life.

421

422 **Acknowledgments**

423 Authors would like to thank the Spanish Ministry of Economy and Competitiveness for
424 financial support (MAT2011-28468-C02-01) and Prof. Juan López Martínez
425 (Polytechnic University of Valencia, Spain) and Prof. José M. Kenny (University of
426 Perugia, Italy) for their support in experimental testing. Marina Ramos would like to
427 thank University of Alicante (Spain) for UAFPU2011-48539721S pre-doctoral research
428 grant.

429

430

ACCEPTED MANUSCRIPT

431 **References**

432

433 (ASTM D 882 - 09. 2009). Standard test method for tensile properties of thin plastic sheeting In: 468
434 Annual book of ASTM standards. Amer. Soc. for Testing & Materials, Philadelphia, PA.

435 Al-Bandak, G., & Oreopoulou, V. (2007). Antioxidant properties and composition of *Majorana syriaca*
436 extracts. *European Journal of Lipid Science and Technology*, 109(3), 247-255.

437 Álvarez, M. F. (2000). Revisión: Envasado activo de los alimentos / Review: Active food packaging Food
438 Science and Technology International, 6(2), 97-108.

439 Byun, Y., Kim, Y. T., & Whiteside, S. (2010). Characterization of an antioxidant polylactic acid (PLA)
440 film prepared with α -tocopherol, BHT and polyethylene glycol using film cast extruder. *Journal of*
441 *Food Engineering*, 100(2), 239-244.

442 Del Nobile, M. A., Conte, A., Buonocore, G. G., Incoronato, A. L., Massaro, A., & Panza, O. (2009).
443 Active packaging by extrusion processing of recyclable and biodegradable polymers. *Journal of*
444 *Food Engineering*, 93(1), 1-6.

445 Fukushima, K., Abbate, C., Tabuani, D., Gennari, M., & Camino, G. (2009a). Biodegradation of
446 poly(lactic acid) and its nanocomposites. *Polymer Degradation and Stability*, 94(10), 1646-1655.

447 Fukushima, K., Tabuani, D., & Camino, G. (2009b). Nanocomposites of PLA and PCL based on
448 montmorillonite and sepiolite. *Materials Science and Engineering: C*, 29(4), 1433-1441.

449 Gamez-Perez, J., Nascimento, L., Bou, J. J., Franco-Urquiza, E., Santana, O. O., Carrasco, F., & Ll.
450 MasPOCH, M. (2011). Influence of crystallinity on the fracture toughness of poly(lactic
451 acid)/montmorillonite nanocomposites prepared by twin-screw extrusion. *Journal of Applied*
452 *Polymer Science*, 120(2), 896-905.

453 Gómez-Estaca, J., Giménez, B., Montero, P., & Gómez-Guillén, M. C. (2009). Incorporation of
454 antioxidant borage extract into edible films based on sole skin gelatin or a commercial fish gelatin.
455 *Journal of Food Engineering*, 92(1), 78-85.

456 Hughes, J., Thomas, R., Byun, Y., & Whiteside, S. (2012). Improved flexibility of thermally stable poly-
457 lactic acid (PLA). *Carbohydrate Polymers*, 88(1), 165-172.

458 Hwang, S. W., Shim, J. K., Selke, S. E. M., Soto-Valdez, H., Matuana, L., Rubino, M., & Auras, R.
459 (2012). Poly(L-lactic acid) with added α -tocopherol and resveratrol: optical, physical, thermal and
460 mechanical properties. *Polymer International*, 61(3), 418-425.

- 461 Inkinen, S., Hakkarainen, M., Albertsson, A.-C., & Sodergard, A. (2011). From Lactic Acid to Poly(lactic
462 acid) (PLA): Characterization and Analysis of PLA and Its Precursors. *Biomacromolecules*, 12(3),
463 523-532.
- 464 Jamshidian, M., Arab Tehrani, E., Cleymand, F., Leconte, S., Falher, T., & Desobry, S. (2012). Effects of
465 synthetic phenolic antioxidants on physical, structural, mechanical and barrier properties of poly
466 lactic acid film. *Carbohydrate Polymers*, 87(2), 1763-1773.
- 467 Lagaron, J. M., & Lopez-Rubio, A. (2011). Nanotechnology for bioplastics: opportunities, challenges and
468 strategies. *Trends in Food Science & Technology*, 22(11), 611-617.
- 469 Lewitus, D., McCarthy, S., Ophir, A., & Kenig, S. (2006). The Effect of Nanoclays on the Properties of
470 PLLA-modified Polymers Part 1: Mechanical and Thermal Properties. *Journal of Polymers and the
471 Environment*, 14(2), 171-177.
- 472 López-Rubio, A., & Lagaron, J. M. (2010). Improvement of UV stability and mechanical properties of
473 biopolyesters through the addition of β -carotene. *Polymer Degradation and Stability*, 95(11), 2162-
474 2168.
- 475 Manzanarez-López, F., Soto-Valdez, H., Auras, R., & Peralta, E. (2011). Release of [alpha]-Tocopherol
476 from Poly(lactic acid) films, and its effect on the oxidative stability of soybean oil. *Journal of Food
477 Engineering*, 104(4), 508-517.
- 478 Martino, V. P., Ruseckaite, R. A., Jiménez, A., & Averous, L. (2010). Correlation between Composition,
479 Structure and Properties of Poly(lactic acid)/Polyadipate-Based Nano-Biocomposites.
480 *Macromolecular Materials and Engineering*, 295(6), 551-558.
- 481 Mastelic, J., Jerkovic, I., Blazevic, I., Poljak-Blazi, M., Borovic, S., Ivancic-Bace, I., Smrecki, V.,
482 Zarkovic, N., Brcic-Kostic, K., Vikić-Topić, D., & Müller, N. (2008). Comparative study on the
483 antioxidant and biological activities of carvacrol, thymol, and eugenol derivatives. *Journal of
484 Agricultural and Food Chemistry*, 56(11), 3989-3996.
- 485 Ortiz-Vazquez, H., Shin, J., Soto-Valdez, H., & Auras, R. (2011). Release of butylated hydroxytoluene
486 (BHT) from Poly(lactic acid) films. *Polymer Testing*, 30(5), 463-471.
- 487 Persico, P., Ambrogi, V., Carfagna, C., Cerruti, P., Ferrocino, I., & Mauriello, G. (2009). Nanocomposite
488 polymer films containing carvacrol for antimicrobial active packaging. *Polymer Engineering &
489 Science*, 49(7), 1447-1455.

- 490 Picard, E., Espuche, E., & Fulchiron, R. (2011). Effect of an organo-modified montmorillonite on PLA
491 crystallization and gas barrier properties. *Applied Clay Science*, 53(1), 58-65.
- 492 Quilaqueo Gutiérrez, M., Echeverría, I., Ihl, M., Bifani, V., & Mauri, A. N. (2012).
493 Carboxymethylcellulose–montmorillonite nanocomposite films activated with murta (*Ugni molinae*
494 Turcz) leaves extract. *Carbohydrate Polymers*, 87(2), 1495-1502.
- 495 Ramos, M., Jiménez, A., Peltzer, M., & Garrigós, M. C. (2012). Characterization and antimicrobial
496 activity studies of polypropylene films with carvacrol and thymol for active packaging. *Journal of*
497 *Food Engineering*, 109(3), 513-519.
- 498 Rhim, J.-W., Hong, S.-I., & Ha, C.-S. (2009). Tensile, water vapor barrier and antimicrobial properties of
499 PLA/nanoclay composite films. *LWT - Food Science and Technology*, 42(2), 612-617.
- 500 Sánchez-Moreno, C. (2002). Review: methods used to evaluate the free radical scavenging activity in
501 foods and biological systems. *Food Science and Technology International*, 8(3), 121-137.
- 502 Scherer, R., & Godoy, H. T. (2009). Antioxidant activity index (AAI) by the 2,2-diphenyl-1-
503 picrylhydrazyl method. *Food Chemistry*, 112(3), 654-658.
- 504 Tabatabaei, S. H., & Aji, A. (2011). Orientation, mechanical, and optical properties of poly (lactic acid)
505 nanoclay composite films. *Polymer Engineering & Science*, 51(11), 2151-2158.
- 506 Viuda-Martos, M., Navajas, Y. R., Zapata, E. S., Fernández-López, J., & Pérez-Álvarez, J. A. (2010).
507 Antioxidant activity of essential oils of five spice plants widely used in a Mediterranean diet.
508 *Flavour and Fragrance Journal*, 25(1), 13-19.
- 509
- 510

511 **Figure captions**

512 **Fig. 1.** TG (a) and DTG (b) curves obtained for pure PLA and nano-biocomposites
513 under nitrogen.

514 **Fig. 2.** Visual observation of PLA and nano-biocomposite films.

515 **Fig. 3.** WAXS patterns of D43B, PLA and nano-biocomposites.

516 **Fig. 4.** TEM images of PLA/T/D43B2.5 nano-biocomposite film.

ACCEPTED MANUSCRIPT

Table 1

Quantification of thymol by HPLC-UV analysis and radical scavenging activity measured by DPPH assay obtained for the different formulations used in this work.

Sample	D43B (wt%)	Thymol (wt%)	Amount of extracted Thymol (wt%) ^a	Inhibition (%) ^b
PLA	-	-	n.d.	n.d.
PLA/D43B2.5	2.5	-	n.d.	n.d.
PLA/D43B5	5	-	n.d.	n.d.
PLA/T	-	8	5.57 ± 0.01	71.1 ± 0.2
PLA/T/D43B2.5	2.5	8	5.99 ± 0.03	84.3 ± 0.3
PLA/T/D43B5	5	8	5.78 ± 0.02	83.5 ± 0.1

^a(n =3, mean ± SD); ^b(n =3, mean ± SD); (n.d.: not detected)

Table 2

TGA and DSC parameters obtained for all nano-biocomposites.

Sample	wt% weight loss (1 st step)	T _{ini} (°C) (2 nd step)	T _{max} (°C) (2 nd step)	T _g (°C)
PLA	n.d.	335	369	57
PLA/D43B2.5	n.d.	334	363	57
PLA/D43B5	n.d.	340	369	57
PLA/T	6.6	331	366	43
PLA/T/D43B2.5	6.3	336	366	41
PLA/T/D43B5	7.1	339	369	44

(n.d.: not detected)

Table 3

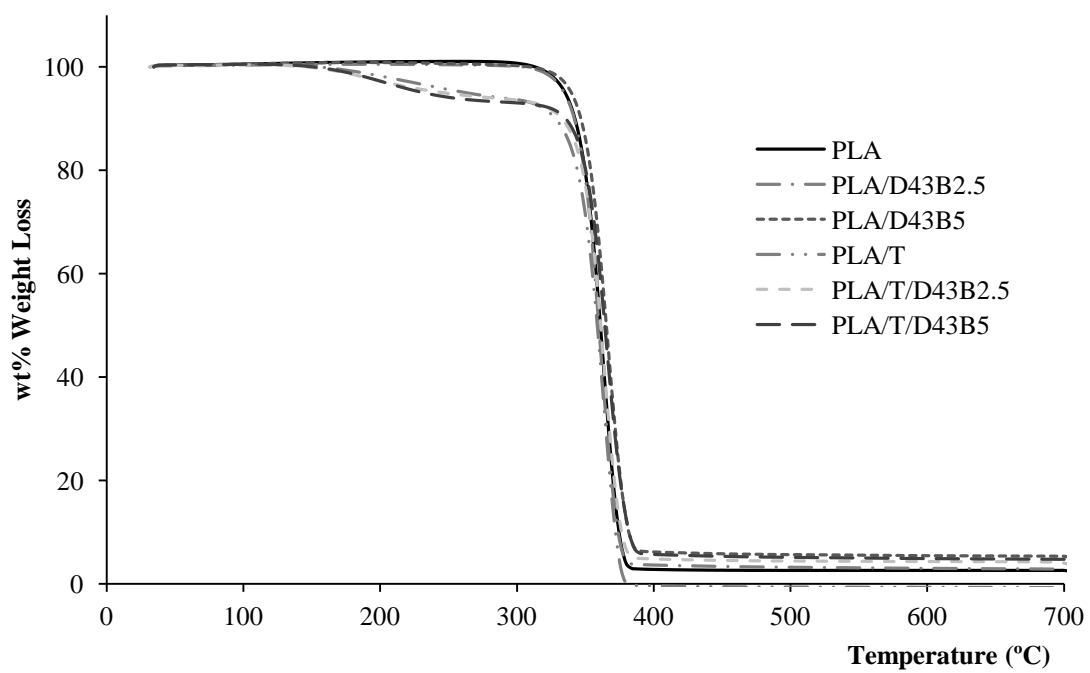
Tensile properties (ASTM D882-09), oxygen transmission rate and CIELab colour parameters obtained for all the studied formulations.

Sample	Elongation at break (%) ^a	Elastic modulus (MPa) ^a	OTR·e (cm ³ mm m ⁻² day) ^b	L*	a*	b*	ΔE* ^c
PLA	3.5 ± 0.1	2575 ± 76	22.1 ± 1.5	30.3	-0.11	-0.20	-
PLA/D43B2.5	2.1 ± 0.4	2739 ± 151	20.1 ± 2.0	30.7	0.02	-0.01	0.5
PLA/D43B5	1.5 ± 0.2	2715 ± 95	17.1 ± 2.3	32.0	-0.24	-0.81	1.9
PLA/T	4.3 ± 0.1	2167 ± 196	23.0 ± 0.2	33.3	-0.49	-1.10	3.2
PLA/T/D43B2.5	2.4 ± 0.1	2246 ± 135	20.1 ± 0.1	32.0	-0.22	-1.14	2.0
PLA/T/D43B5	2.4 ± 0.2	2140 ± 116	22.7 ± 1.3	34.4	-0.58	-1.48	4.4

^a n = 5, mean ± SD
^b n = 3, mean ± SD (e: thickness, mm)
^c PLA film was used as control

Fig. 1

(a)



(b)

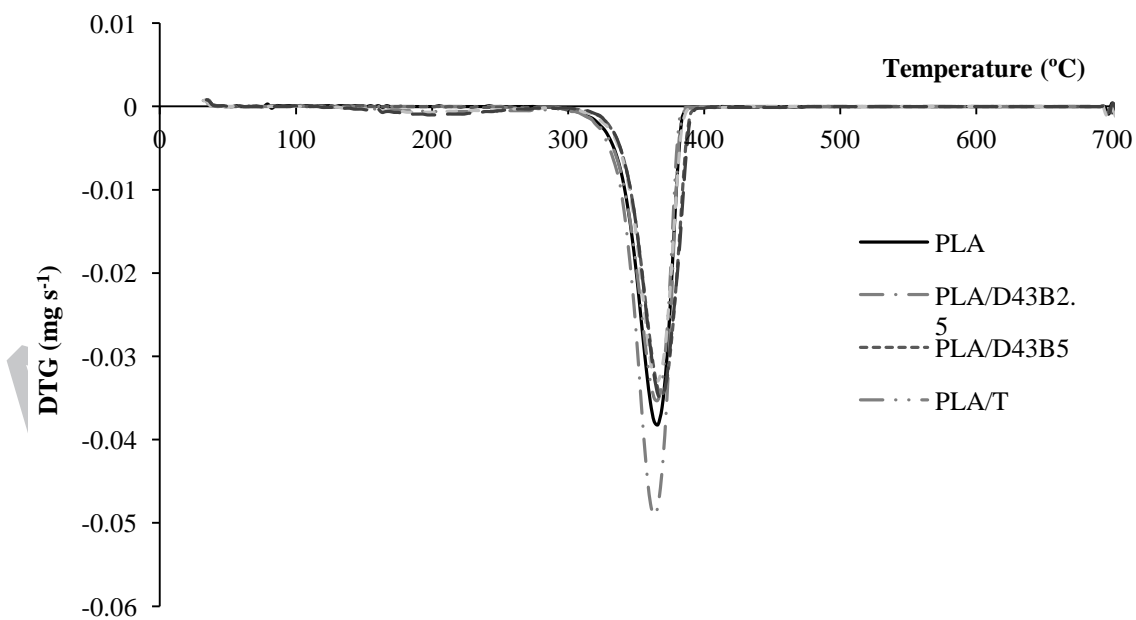


Fig. 2

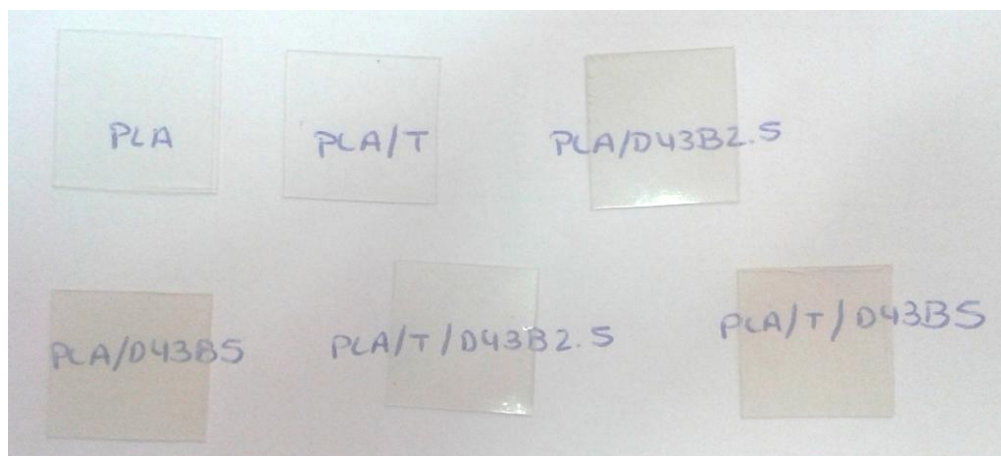


Fig. 3

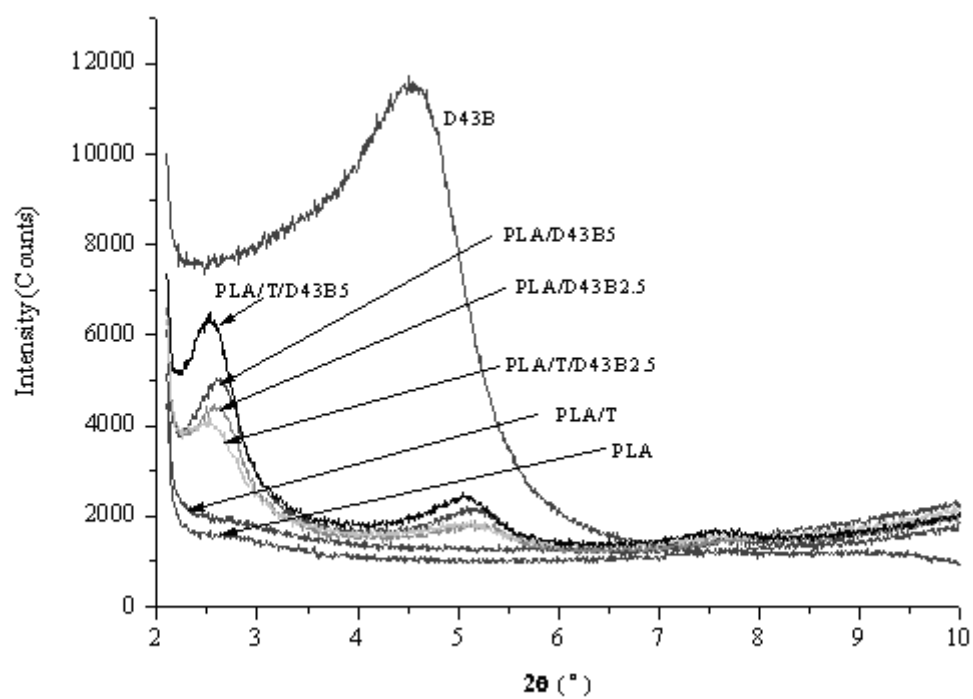
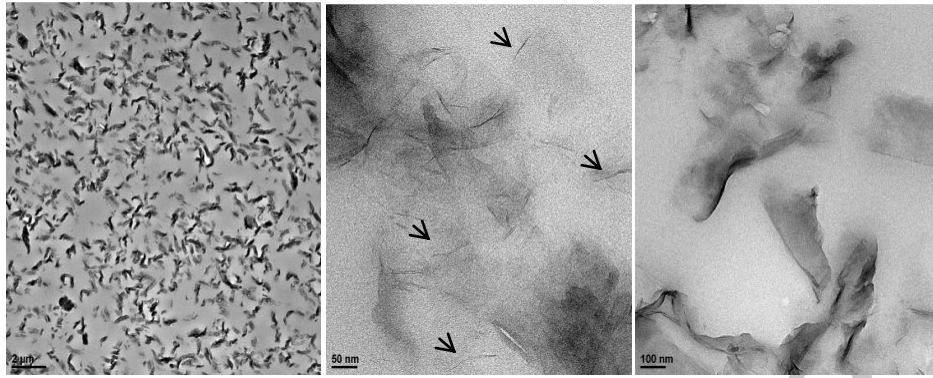


Fig. 4



Highlights

1. Thymol and D43B were added to PLA to get antioxidant nano-biocomposite films
2. A full characterization of all formulations was carried out
3. The presence of thymol in the films and its antioxidant activity were demonstrated
4. The addition of D43B improved oxygen barrier and mechanical properties of films
5. The film with thymol and 2.5 wt% of D43B was considered the best enhanced material